Materials Research Proceedings **26** (2023) 281-286 https://doi.org/10.21741/9781644902431-46

Numerical simulation of coronary arteries blood flow: effects of the aortic valve and boundary conditions

Seyyed Mahmoud Mousavi[1, a *], Gianluca Zitti[1, b], Marco Pozzi[2,c] and Maurizio Brocchini[1, d]

[1]Department of Construction, Civil Engineering, and Architecture, Polytechnic University of Marche, Ancona, Italy

[2]Department of Pediatric and Congenital Cardiac Surgery and Cardiology, United Hospital, Ancona, Italy

[a]s.m.mousavi@pm.univpm.it, [b]g.zitti@staff.univpm.it, [c]marco.pozzi@ospedaliriuniti.marche.it, [d]m.brocchini@staff.univpm.it

* Corresponding author, (s.m.mousavi@pm.univpm.it)

Keywords: Coronary Perfusion, Aortic Valve, Boundary Conditions, Numerical Simulation

Abstract. Sudden cardiac death in athletes is often related to anomalies in coronary origin, which may affect how coronary arteries supply blood to the heart; this highlights the importance of understanding coronary perfusion. Studies for the simulation and predictions of coronary blood flow under normal or disease conditions are many. Numerical simulations can provide rich information about the coronary blood flow with reduced costs in relation to physical models. Correct numerical simulation of the coronary blood flow is still challenging due to the complex interactions with the upstream, e.g., the aortic root, and downstream, e.g., the ventricular contraction, parts of the coronary arteries. Among all, the intrinsic ability of coronary artery autoregulation, intramyocardial resistance, cardiac frequency, and aortic valve functioning could significantly affect the coronary artery perfusion. In the present study, we aim at investigating the effects of the aortic valve and boundary conditions on coronary perfusion. We numerically modeled, by means of the ANSYS-Fluent software, the blood flow inside the proximal parts of the left and right coronary arteries, aortic sinuses of Valsalva, and ascending aorta with and without the aortic valve; the geometry of the computational model represents the average healthy person. Physiological boundary values have been applied at the computational domain boundaries to achieve a stable solution of the Navier-Stokes equations, which govern the incompressible, laminar, Newtonian blood flow. Our numerical results give insight into a proper numerical setup to predict coronary blood flow.

Introduction

The main medical cause of death in athletes is sudden cardiac death (SCD) [1]. High risks of SCD have been observed among patients with a history of coronary artery disease (CAD) [2]. There are multiple research studies in the literature indicating the possible relations between coronary abnormal functioning and myocardial ischemia which might lead to SCD [3,4]. Thus, knowing about coronary artery perfusion could help coronary artery disease diagnosis and surgical planning prior to SCD.

While medical imaging is applied widely for cardiovascular and coronary artery diagnosis, they show no predictive capabilities particularly in pathology of the anomalous course of the coronary artery in SCD [5,6]. Alternatively, computational methods provide this opportunity to virtually simulate the cardiovascular system including the coronary arteries. Lumped parameter or one-dimensional computational models have been successfully hired to study the variety of patient-

specific blood flow simulations [7–9]. However, these methods cannot suitably model pressure wave propagations or fluid-structure interaction phenomena, which are important factors in arterial blood flow simulations [10], such as in the aortic root and proximal part of the coronary arteries. Thus, 3D computational fluid dynamics (CFD) simulations, particularly when they are coupled with the structural models, can provide a detailed analysis of the blood flow in coronary arteries.

In this paper, we simulate the blood flow in a three-dimensional model of the proximal parts of the left and right coronary arteries, aortic sinuses of Valsalva, and ascending aorta of average healthy people. We applied physiological pressure and flow rate boundary values at the boundary locations of the computational domain. Subsequently, a numerical flexible aortic valve model has been integrated into the computational domain of the blood volume to study the effects of the aortic valve functioning on coronary artery perfusion.

Methods

The computational domain is twofold. One is the blood volume, and the other is the aortic valve structural model.

We follow the descriptions of works by [11–13] to design the blood flow computational volume that represents average healthy people. The blood volume consists of the inlet volume (included to manage the inflow), the aortic sinuses of Valsalva, proximal parts of the left and right coronary arteries, and the ascending aorta which are shown in Fig. 1; the dimensions of the model elements are reported in Table 1.

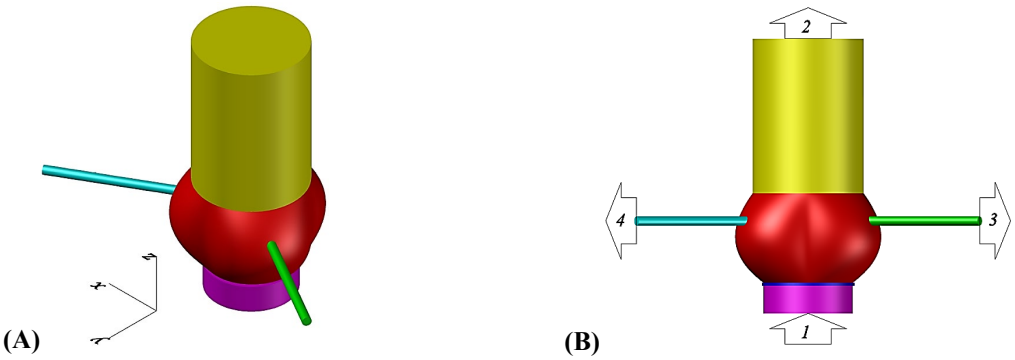

(A) **(B)**

Fig. 1 (A) 3D schematic of the blood volume computational domain including inlet aorta (magenta), aortic sinuses of Valsalva (red), ascending aorta (yellow), left (green), and right (blue) coronary arteries. (B) Numbers showing the flow domain boundary locations, (1) inlet, (2) aorta outlet, (3) left coronary outlet, and (4) right coronary outlet.

Table 1 The dimensions of the flow volume computational domain elements as shown in Fig. 1.

No	Part	Length [mm]	Diameter [mm]
1	Ascending aorta	50	36
2	Left and right coronary arteries	40	3
3	Sinuses of Valsalva	29	29 (aortic annulus) 36 (sinotubular junction)
4	Inlet aorta	10	29

Moreover, the computational flow domain is integrated into the aortic valve structural model that is shown in Fig. 2-A. The aortic valve is located right after the aortic inlet downstream at the location of the aortic annulus, see Fig. 2-B. The design of the numerical model of the aortic valve mimics fairly well the geometry of the Medtronic Avalus 400 bioprosthetic aortic valve that is shown in Fig. 2-C; the corresponding dimensions of the aortic valve model are reported in Table 2. The dynamics of the fluid and solid parts of the domain have been simulated with the numerical software Ansys® Fluent and Ansys® Transient Structural, respectively, coupled in a solver

package that iteratively solves the discretized forms of the governing equations of the fluid flow and solid motion at each computational mesh point. The mesh characteristics of the computational domain are summarized in Table 3.

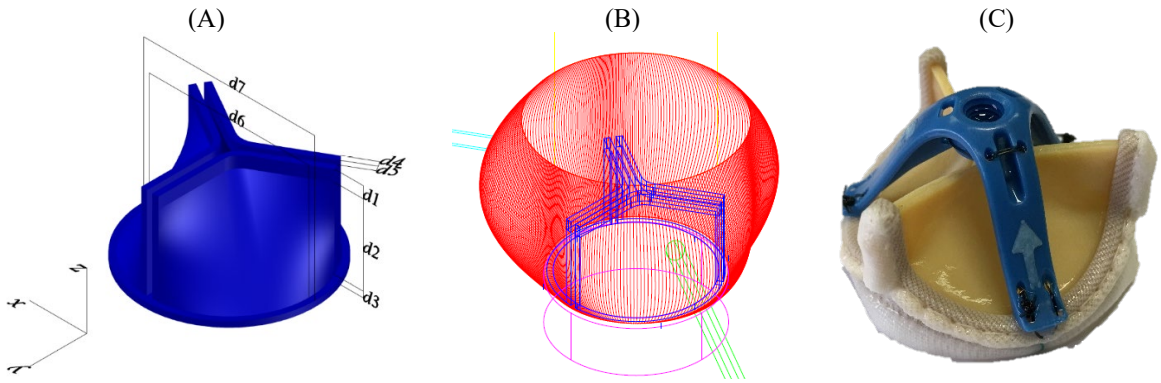

Fig. 2. The aortic valve computational domain (A) is located downstream of the aortic inlet (magenta) at the aortic annulus (red) center (B), which has been designed according to the Medtronic Avalus 400 bioprosthetic aortic valve (C).

The fluid flow governing equations are the principle of mass conservation and the Navier-Stokes equations for incompressible fluid, characterized by density of $\rho = 1060[kg/m^3]$ and dynamic viscosity of $\mu = \nu \times \rho = 3.5 \times 10^{-3}\ [Pa.s]$ [14]. The motion of the aortic valve with flexible leaflets is governed by the linear momentum balance equation, considering a linear elastic and isotropic material, with the Young's modulus of $1[MPa]$, Poisson's ratio of 0.45, and density $\rho_s = 1000[kg/m^3]$, in line with previous studies [15,16]. The equilibrium of surface forces is applied at the interface between the solid and fluid parts of the domain.

Table 2 Dimensions of the computational aortic valve structural model elements according to the parameters shown in Fig. 2-A.

No	Part	Dimension $[mm]$
1	$d1$	2
2	$d2$	14
3	$d3$	1
4	$d4$	1
5	$d5$	1
6	$d6$	28
7	$d7$	30

Table 3 Summary of the computational domain mesh characteristics generated in ANSYS.

Computational domain	Element type	Element order	Number of nodes	Number of elements	Min element size $[m]$	Max element size $[m]$
Blood volume	Tetrahedral	Linear	71248	389719	4.9063e-05	0.00887179
Aortic valve	Tetrahedral	Linear	665	1617	4.2214e-04	4.5706e-03

Results and Discussion

To evaluate the effect of inlet boundary value, we applied two sets of boundary conditions: the first set of boundary conditions (called *inlet flow*), taken from reference [17], are a physiological aortic flow rate at the inlet volume, and physiological pressure values at three other outlets; the second set (called *inlet pressure*), evaluated from reference [14], are the physiological left ventricular pressure at the inlet volume and three physiological pressure values at three outlet boundary locations. Moreover, the role of the aortic valve is studied considering two numerical

Materials Research Proceedings **26** (2023) 281-286 https://doi.org/10.21741/9781644902431-46

model configurations: one configuration simulates merely the blood volume computational domain, without the valve (called *without valve*) and the other is the fluid-structure interaction of the blood volume with the aortic valve structural model (called *with valve*).

Fig. 3-A and Fig. 3-B, show respectively the calculated numerical flow rate values of the left and right coronary arteries when we hired the *inlet flow* boundary conditions. In each panel of the figure, we can compare the results of the configuration *without valve* (shown in blue) and of the one *with valve* (shown in yellow) to the reference values (shown in orange) borrowed from [17].

Moreover, the numerical results of the left and right coronary artery flow rates when we applied the *inlet pressure* boundary conditions from [14] are shown in Fig. 4-A and Fig. 4-B respectively. Similar to the former case, the blue color shows the results of the configuration *without valve* and yellow indicates the results of the model *with valve*.

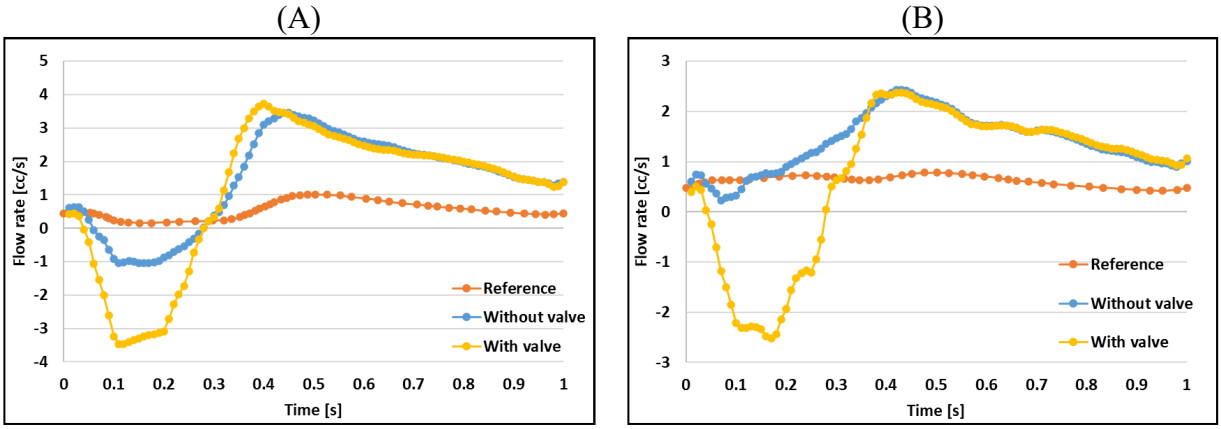

Fig. 3. (A) Left and (B) right coronary artery flow rates when we applied physiological aortic flow rate at the inlet volume boundary location and physiological pressure values at three outlet boundary locations; all boundary values are hired from reference [17].

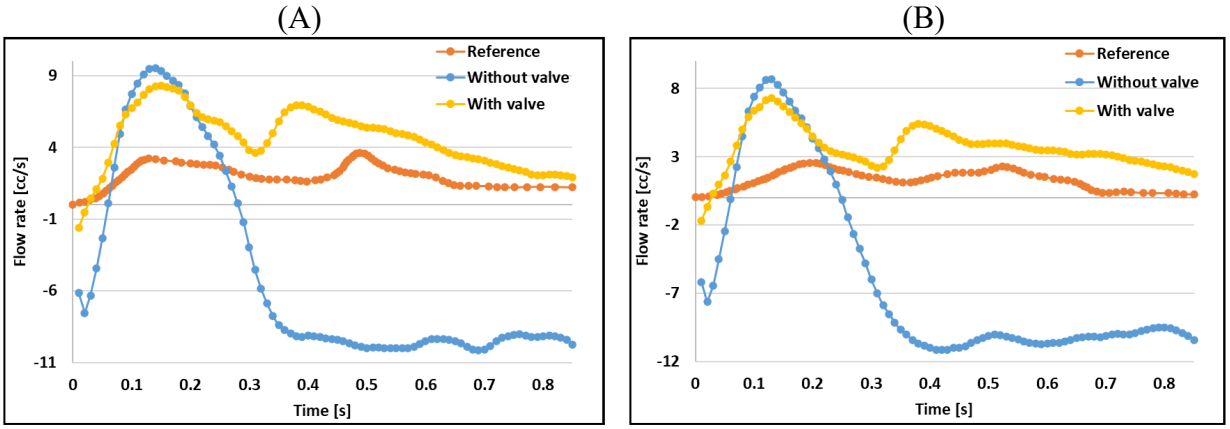

Fig. 4. (A) Left and (B) right coronary artery flow rate when we applied physiological pressure values at the aorta inlet boundary location as well as physiological pressure values at three outlet boundary locations; all boundary values are hired from reference [14].

By comparing the numerical results of the models *without valve* in Fig. 3 and Fig. 4, we can observe that the model with the *inlet flow* boundary conditions could better simulate the coronary artery perfusion compared to the model with the *inlet pressure* boundary conditions. In other words, the calculated coronary perfusion waveforms in the former model are mostly positive values following, though not perfectly, the waveforms of the reference values. In contrast, the

numerical coronary artery flow rates in the latter model show large negative values, particularly in the diastolic phase. However, the results of the model *without valve* by applying either set of the boundary conditions show deviation from their corresponding reference values. Thus, we run the simulations *with valve* to study the role of the aortic valve functioning in coronary artery perfusion. The comparison of the results obtained in models with and without valve in Fig. 3 indicates that the inclusion of the aortic valve in the numerical model does not improve the calculated coronary flow rates when the flow rate inlet boundary condition is used. This might be due to the fact that the inlet volume flow rate boundary condition reported in reference [17] is located downstream of the aortic valve. On contrary, in our numerical model, the inlet volume boundary location is upstream of the aortic valve, see Fig. 1-B and Fig. 1-B. Nonetheless, the results of the simulation *with valve* in Fig. 4 show that the left and right coronary artery flow rates better resemble the reference values compared to the corresponding simulations *without valve*, if pressure inlet boundary condition is hired.

Conclusion

We numerically studied the effects of boundary conditions and aortic valve functioning on coronary artery flow rates. We could observe that the choice of upstream boundary condition plays a significant role in coronary perfusion. Particularly, considering the model without valve, the *inlet flow* boundary condition provides better results than the *inlet pressure* boundary conditions. Instead, if the aortic valve is included, the *inlet pressure* boundary condition helps better simulate the coronary flow rates. In fact, in real human hearts, the left ventricular pressure acts on the upstream side of the aortic valve.

References

[1] K. G. Harmon, J. A. Drezner, M. G. Wilson, and S. Sharma, "Incidence of sudden cardiac death in athletes: a state-of-the-art review," *Heart*, vol. 100, no. 16, pp. 1227–1234, 2014. https://doi.org/10.1136/heartjnl-2014-093872.rep

[2] A. Rohila and A. Sharma, "Detection of sudden cardiac death by a comparative study of heart rate variability in normal and abnormal heart conditions," *Biocybern. Biomed. Eng.*, vol. 40, no. 3, pp. 1140–1154, 2020. https://doi.org/10.1016/j.bbe.2020.06.003

[3] A. P. Burke, A. Farb, R. Virmani, J. Goodin, and J. E. Smialek, "Sports-related and non-sports-related sudden cardiac death in young adults," *Am. Heart J.*, vol. 121, no. 2, pp. 568–575, 1991. https://doi.org/10.1016/0002-8703(91)90727-Y

[4] A. J. Taylor, K. M. Rogan, and R. Virmani, "Sudden cardiac death associated with isolated congenital coronary artery anomalies," *J. Am. Coll. Cardiol.*, vol. 20, no. 3, pp. 640–647, 1992. https://doi.org/10.1016/0735-1097(92)90019-J

[5] M. C. de Jong, T. S. S. Genders, R.-J. van Geuns, A. Moelker, and M. G. Hunink, "Diagnostic performance of stress myocardial perfusion imaging for coronary artery disease: a systematic review and meta-analysis," *Eur. Radiol.*, vol. 22, no. 9, pp. 1881–1895, 2012. https://doi.org/10.1007/s00330-012-2434-1

[6] M. Kadem, L. Garber, M. Abdelkhalek, B. K. Al-Khazraji, and Z. Keshavarz-Motamed, "Hemodynamic modeling, medical imaging, and machine learning and their applications to cardiovascular interventions," *IEEE Rev. Biomed. Eng.*, p. 1, 2022. https://doi.org/10.1109/RBME.2022.3142058

[7] I. E. Vignon-Clementel, C. Alberto Figueroa, K. E. Jansen, and C. A. Taylor, "Outflow boundary conditions for three-dimensional finite element modeling of blood flow and pressure in

arteries," *Comput. Methods Appl. Mech. Eng.*, vol. 195, no. 29, pp. 3776–3796, 2006. https://doi.org/10.1016/j.cma.2005.04.014

[8] H. J. Kim, I. E. Vignon-Clementel, J. S. Coogan, C. A. Figueroa, K. E. Jansen, and C. A. Taylor, "Patient-specific modeling of blood flow and pressure in human coronary arteries," *Ann. Biomed. Eng.*, vol. 38, no. 10, pp. 3195–3209, 2010. https://doi.org/10.1007/s10439-010-0083-6

[9] M. Mirramezani and S. C. Shadden, "A Distributed Lumped Parameter Model of Blood Flow," *Ann. Biomed. Eng.*, vol. 48, no. 12, pp. 2870–2886, 2020, doi: 10.1007/s10439-020-02545-6. https://doi.org/10.1007/s10439-020-02545-6

[10] M. Mirramezani and S. C. Shadden, "Distributed lumped parameter modeling of blood flow in compliant vessels," *J. Biomech.*, vol. 140, p. 111161, 2022. https://doi.org/10.1016/j.jbiomech.2022.111161

[11] H. Reul, A. Vahlbruch, M. Giersiepen, T. H. Schmitz-Rode, V. Hirtz, and S. Effert, "The geometry of the aortic root in health, at valve disease and after valve replacement," *J. Biomech.*, vol. 23, no. 2, pp. 181–191, 1990. https://doi.org/10.1016/0021-9290(90)90351-3

[12] J. T. Dodge Jr, B. G. Brown, E. L. Bolson, and H. T. Dodge, "Intrathoracic spatial location of specified coronary segments on the normal human heart. Applications in quantitative arteriography, assessment of regional risk and contraction, and anatomic display.," *Circulation*, vol. 78, no. 5, pp. 1167–1180, 1988. https://doi.org/10.1161/01.CIR.78.5.1167

[13] J. T. Dodge, B. G. Brown, E. L. Bolson, and H. T. Dodge, "Lumen diameter of normal human coronary arteries. Influence of age, sex, anatomic variation, and left ventricular hypertrophy or dilation.," *Circulation*, vol. 86, no. 1, pp. 232–246, Jul. 1992. https://doi.org/10.1161/01.CIR.86.1.232

[14] S. Nobari, R. Mongrain, R. Leask, and R. Cartier, "The effect of aortic wall and aortic leaflet stiffening on coronary hemodynamic: a fluid–structure interaction study," *Med. Biol. Eng. Comput.*, vol. 51, no. 8, pp. 923–936, 2013. https://doi.org/10.1007/s11517-013-1066-1

[15] G. Marom, R. Haj-Ali, E. Raanani, H.-J. Schäfers, and M. Rosenfeld, "A fluid–structure interaction model of the aortic valve with coaptation and compliant aortic root," *Med. Biol. Eng. Comput.*, vol. 50, no. 2, pp. 173–182, 2012. https://doi.org/10.1007/s11517-011-0849-5

[16] H. E. Salman, L. Saltik, and H. C. Yalcin, "Computational Analysis of Wall Shear Stress Patterns on Calcified and Bicuspid Aortic Valves: Focus on Radial and Coaptation Patterns," *Fluids* , vol. 6, no. 8. 2021. https://doi.org/10.3390/fluids6080287

[17] M. Yin, A. Yazdani, and G. E. Karniadakis, "One-dimensional modeling of fractional flow reserve in coronary artery disease: Uncertainty quantification and Bayesian optimization," *Comput. Methods Appl. Mech. Eng.*, vol. 353, pp. 66–85, 2019. https://doi.org/10.1016/j.cma.2019.05.005